SUPPORTING INFORMATION

Macroscale Ceramic Origami Structures with Hyper-elastic Coating

Md Shajedul Hoque Thakur[1,2], Methu Dev Nath[3], Pulickel M. Ajayan[2], Glaucio H. Paulino[4], Muhammad M. Rahman*[1,2]

[1]Department of Mechanical and Aerospace Engineering, University of Houston, Houston, TX, USA
[2]Department of Materials Science and NanoEngineering, Rice University, Houston, TX, USA
[3]Department of Mechanical Engineering, Carnegie Mellon University, Pittsburgh, PA, USA
[4]Department of Civil and Environmental Engineering, Princeton University, Princeton, NJ, USA

*Corresponding Author
Email: maksud@uh.edu

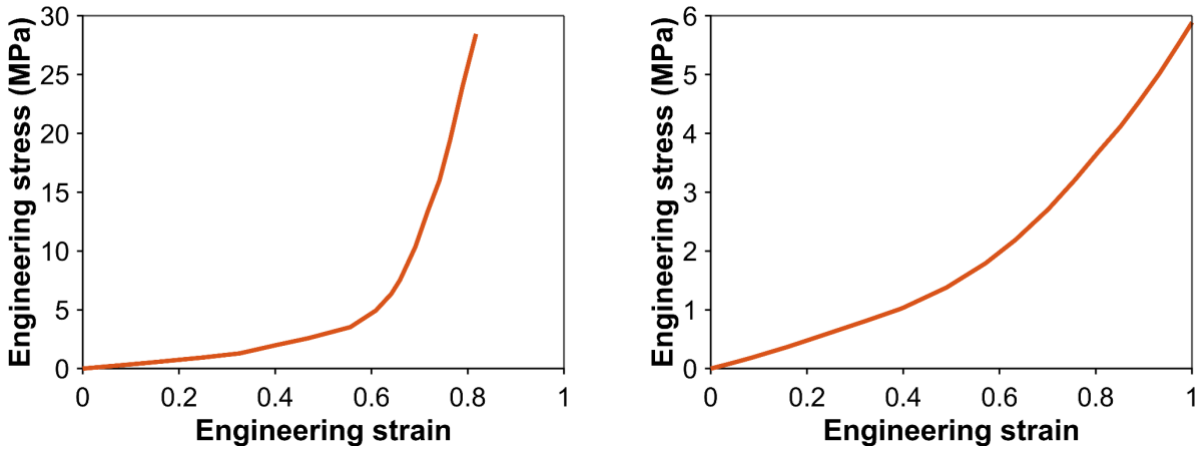

Figure S1. Engineering stress-strain behavior of PDMS (bulk Sylgard 184): uniaxial (a) compression and (b) tension test results.[1]

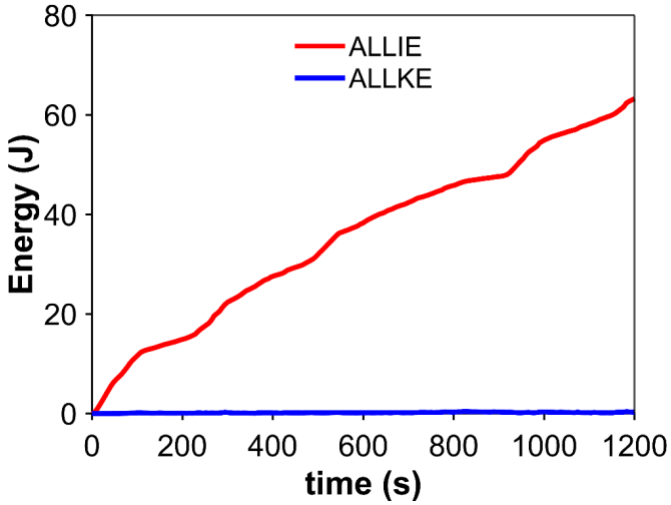

Figure S2. Variation of total kinetic energy (ALLKE) and internal energy (ALLIE) of all coated origami structure elements with time over the entire simulation for quasi-static monotonic compression of coated structure in the X-direction.

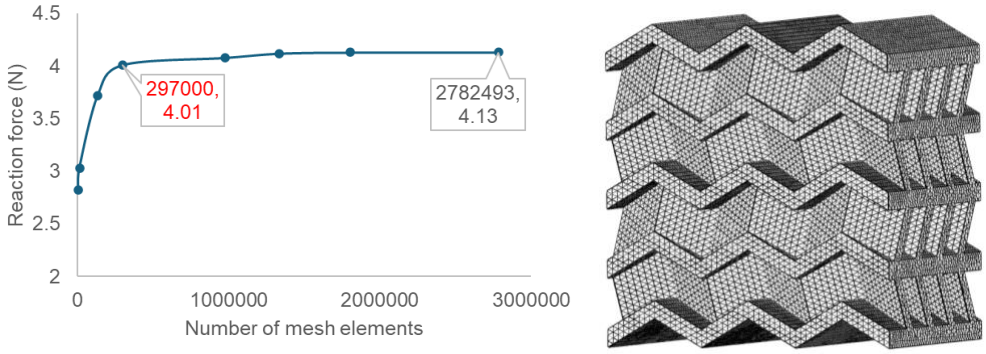

Figure S3. Mesh convergence. The reaction force at an arbitrary node is plotted for various numbers of mesh elements from extremely coarse to extremely fine. The chosen mesh size, 297000, is highlighted in red. Beyond this point, the variation in reaction force with increasing mesh size is less than 5%. Hence 297000 is an appropriate number of mesh elements that gives accurate results within reasonable computational cost. The final mesh used in the study is presented on the right.

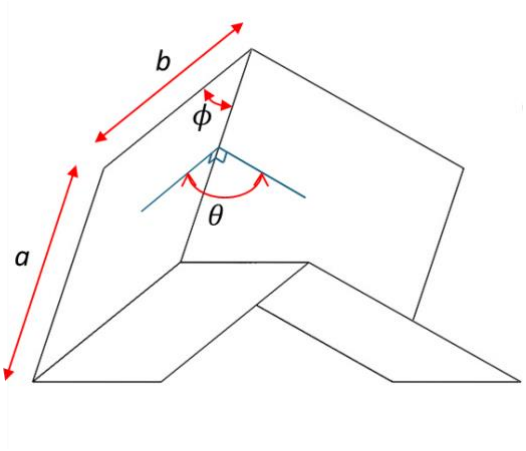

Figure S4. A Miura-ori unit cell with the four independent dimensions labeled: two-panel lengths (*a* and *b*), sector angle ϕ, and folding angle θ.

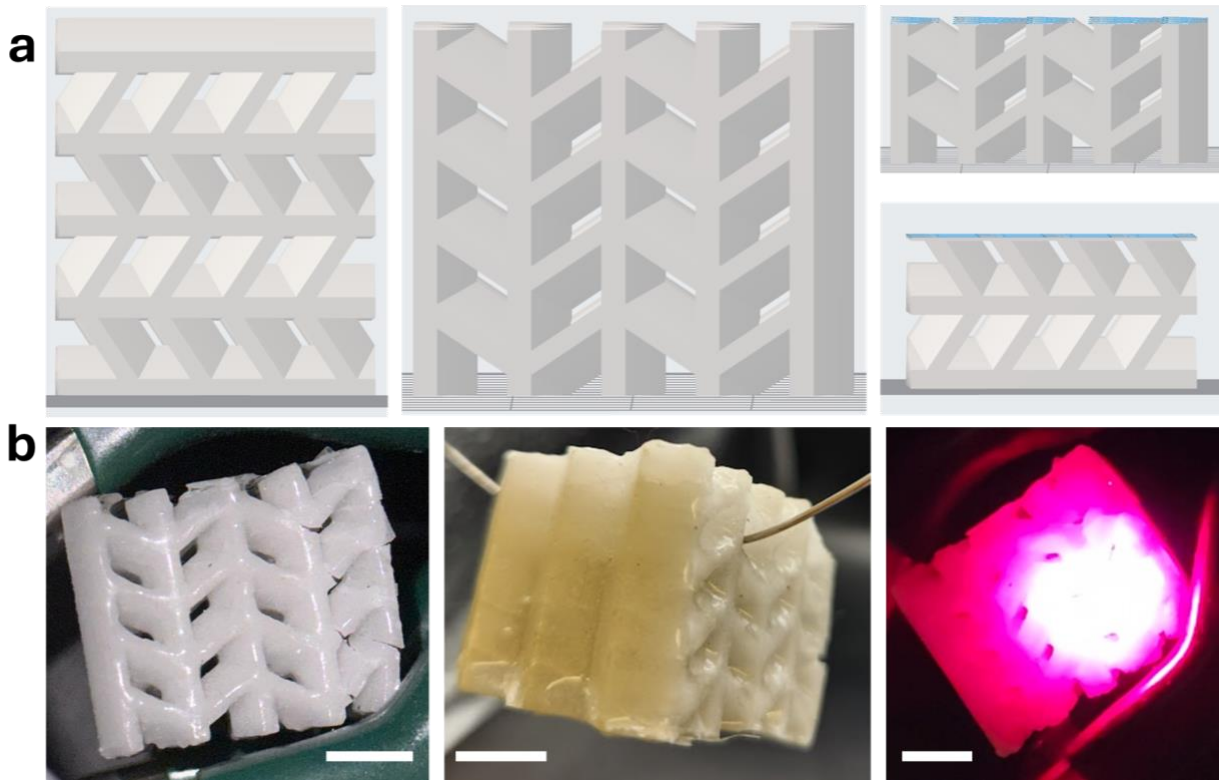

Figure S5. **(a)** Front views and cross-sectional views of the 3D model show the hollow nature of this geometry with direct front-to-back visibility. **(b)** Close-up photographs of the PDMS coated 3D printed origami ceramic structure, demonstrating the hollow nature of the structure. In the first picture, the black background is clearly visible. The next picture shows a metal wire passing through the coated structure, and the third picture shows laser light highlighting the gaps in the structure in a dark environment. Scale bars are 10 mm.

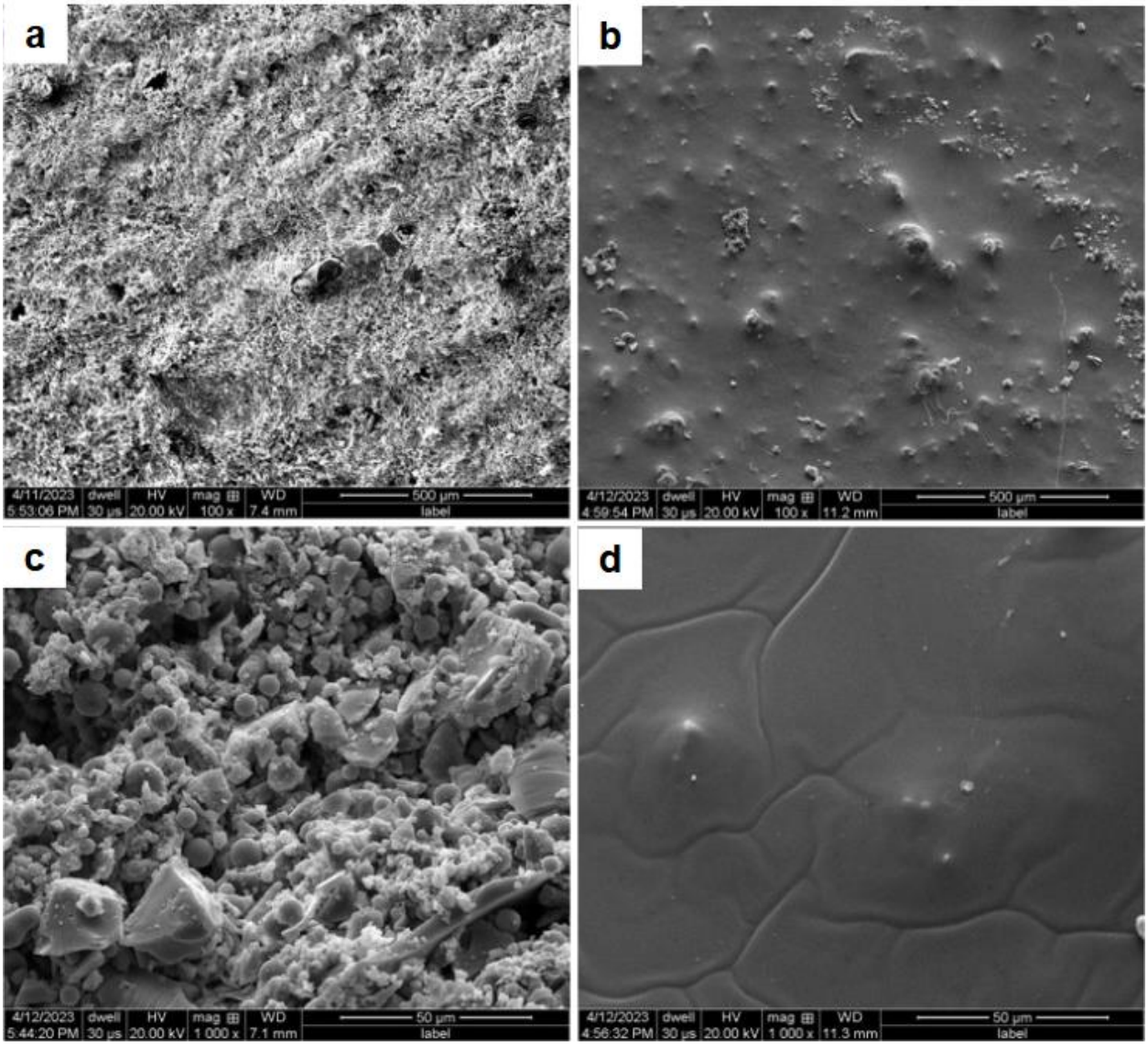

Figure S6. **SEM images of 3D printed ceramic. (a and c)** Before sintering, no layer lines are seen, showing isotropic printed structure. **(b and d)** After sintering, the final consolidated structure also does not show any anisotropy.

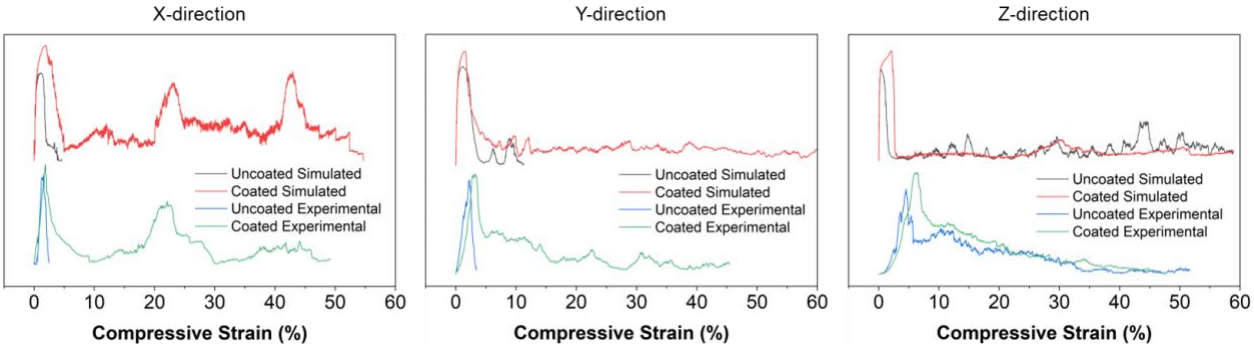

Figure S7. Comparison of the trends between results from simulations and experiments for both coated and uncoated structures. Despite the difference in force magnitudes, the peaks are reached at similar strains, and the overall trends are very similar between experiments and simulations.

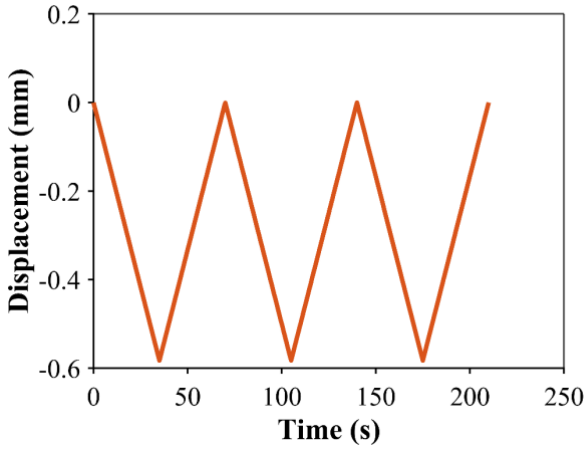

Figure S8. Variation of displacement of the compressing jaw with time for the quasi-static cyclic compression test (FEA).

Supplementary Movie 1. Video depicting the assembly of the 3D origami structure: starting with a single-unit cell, forming a Miura sheet by repeating three cells, creating a tube by attaching a mirror image, and assembling in aligned and zipper couplings to construct the final multi-tube 3D Miura-ori structure.

Table S1. Dimensions of the designed origami structure.

Dimensions (mm)			
X	Y	Z	Panel thickness
36.58	30.38	33.94	2

Table S2. Ceramic resin firing schedule.

Temperature (°C)	Time to temperature (min)	Total time (h)	Phase
0	0	0	Ramp 1
240	240	4	
240	480	12	Burnout hold
300	60	13	
300	60	14	
1271	333	19.5	Ramp 2
1271	10	19.7	Sintering Hold
900	60	20.7	Cool Down
0	900	35.7	

Table S3. Dimensions of the 3D-printed origami structure.

	X	Y	Z
Length (mm)	31.71	26.08	29.61

Table S4. Concrete damaged plasticity model flow parameters used to model the sintered silica ceramic.

Parameter	value	Equation
Dilation angle	31	Eq. (5)
Eccentricity	0.1	Eq. (5)
σ_{b0}/σ_{c0}	1.16	Eq. (2)
K_c	0.66	Eq. (4)

Table S5. Mechanical properties of the sintered silica ceramic used in the experiment and simulation.[2]

Property	Value
Elastic Modulus	50 GPa
Tensile Strength	33.5 MPa
Compressive strength	90 MPa
Density	1.9 gcm^{-3}

Table S6. Yield stress and the corresponding inelastic strain of the ceramic (silica) under uniaxial compressive loading.

$\boldsymbol{\sigma_y}$ (MPa)	$\boldsymbol{\varepsilon_{in}}$
90	0
69.3	0.01
49.5	0.02
29.7	0.05
9.9	0.1
0.9	1

Table S7. Damage parameter and the corresponding inelastic strain of the ceramic (silica) under uniaxial compressive loading.

d	ε_{in}
0	0
0.2	0.01
0.5	0.02
0.9	0.05
0.9	1

Table S8. Yield stress and the corresponding cracking strain of the ceramic (silica) under uniaxial tensile loading.

σ_y (MPa)	ε_{in}
33.5	0
23.5	0.1
13.5	0.2
3.5	0.5

Table S9. Damage parameter and the corresponding cracking strain of ceramic (silica) under uniaxial tensile loading.

d	ε_{in}
0	0
0.299	0.1
0.597	0.2
0.896	0.5

Table S10. Arruda- Boyce model parameters used to model the PDMS in the coating.

Parameter	Value
μ	0.983
λ_m	1.005
D	5.270

References

[1] I. D. Johnston, D. K. McCluskey, C. K. L. Tan, M. C. Tracey, *J. Micromech. Microeng.* **2014**, *24*, 035017.

[2] S. M. Sajadi, L. Vásárhelyi, R. Mousavi, A. H. Rahmati, Z. Kónya, Á. Kukovecz, T. Arif, T. Filleter, R. Vajtai, P. Boul, Z. Pang, T. Li, C. S. Tiwary, M. M. Rahman, P. M. Ajayan, *Sci. Adv.* **2021**, *7*, eabc5028.